NASA CR -112230

A PARAMETRIC STUDY OF PLANFORM AND AEROELASTIC EFFECTS ON AERODYNAMIC CENTER, a- AND q- STABILITY DERIVATIVES

APPENDIX B

METHOD FOR COMPUTING THE STRUCTURAL INFLUENCE COEFFICIENT MATRIX OF NONPLANAR WING-BODY-TAIL CONFIGURATIONS

by

J. Roskam, H. Smith, and G. Gibson

CRINC-FRL 72-012

October 1972

Prepared under NASA Grant NGR 17-002-071 by

The Flight Research Laboratory
Department of Aerospace Engineering
The University of Kansas
Lawrence, Kansas 66044

for

Langley Research Center
National Aeronautics and Space Administration

TABLE OF CONTENTS

1. INTRODUCTION

The purpose of this appendix is to explain the method used in computing the structural influence coefficient matrix (or [C] matrix) of the computer program of Reference 1 (Appendix A of the Summary Report). This [C] matrix is computed for complete wing-body-tail configurations as shown in Figure 1 by assuming that all major airplane components can be structurally represented by a slender beam called the elastic axis. Referring to Figure 1, a structural influence coefficient (i.e. any element C_{jk} of matrix [C]) is defined as the rotation about the Y-stability axis at panel "j" induced by a unit load on panel "k". Symbols used in this appendix are defined in Section 2. A description of how a structural breakdown is performed in detail is presented in Section 3. The method used in computing the elements of the structural influence coefficient matrix, [C], is developed in Section 4. Validation of this method is discussed in Section 5.

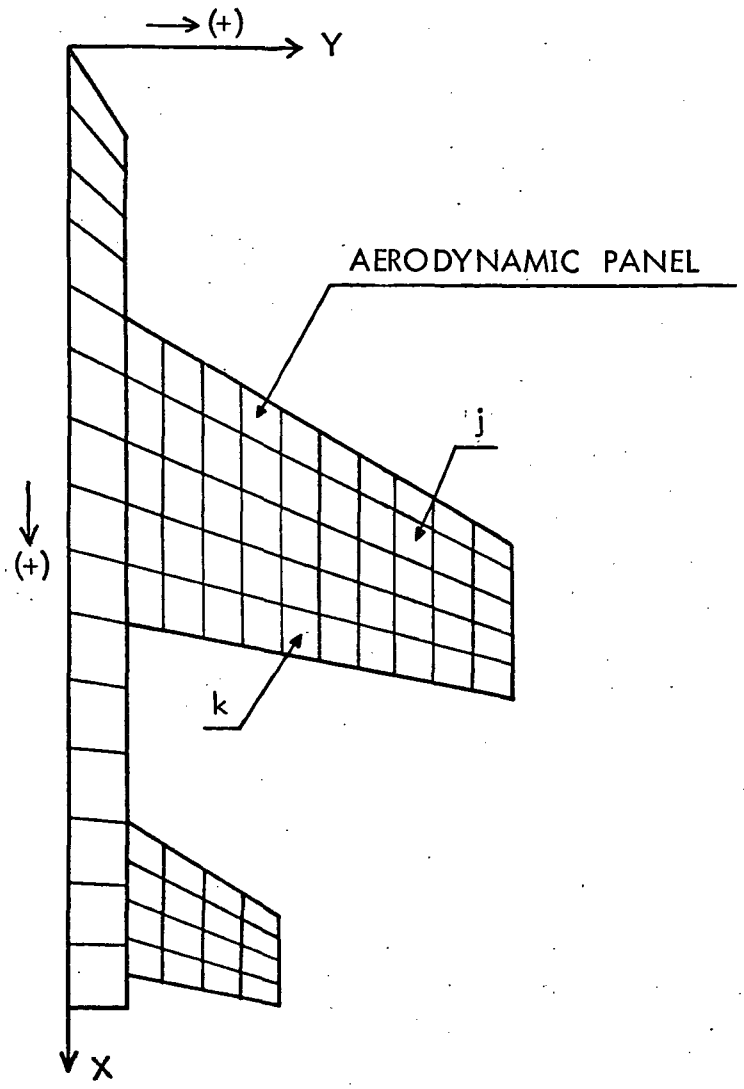

(a) Example of Paneled Airplane Configuration

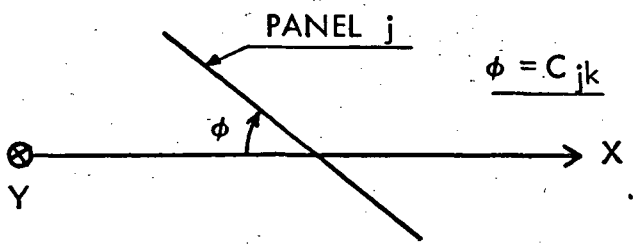

(b) Definition of C_{jk}

Figure 1 Definition of Elements of the Structural Influence Coefficient Matrix

2. SYMBOLS

The units used for the physical quantities defined in this paper are given both in the International System of Units (SI) and the U.S. Customary Units.

Symbol	Definition	Dimension
$[C]$	structural influence coefficient matrix	rad./lb (rad./N.)
C_{jk}	structural influence coefficient (change in angle of attack of panel j due to a unit load on panel k)	rad./lb. (rad./N.)
c_s	structural root chord	in.(m)
c.p.	panel center of pressure	
EI	bending stiffness	lb.-in.^{2} (N.-m^2)
GJ	torsional stiffness	lb.-in.^{2} (N.-m^2)
L_i	length of i-th elastic axis segment	in.(m)
M	moment	in-lb.(m.-N.)
P	force	lb. (N.)
T	torque	in-lb.(m.-N.)
α	total streamwise rotation (angle of attack) of a point on the elastic axis	rad.
$\Delta\alpha$	change in streamwise angle of attack of an elastic axis segment	rad.

Symbol	Definition	Dimension
γ_i	sweep angle of i-th elastic axis segment	rad.
θ_M	bending angle due to a bending moment	rad.
θ_T	bending angle due to a torque	rad.
ϕ_M	twist angle due to a bending moment	rad.
ϕ_T	twist angle due to a torque	rad.

3. DESCRIPTION OF STRUCTURAL BREAKDOWN

For purposes of analysis, the entire internal structure of the airplane is reduced to a number of elastic axes. For example, the elastic axis of the wing becomes a cantilever beam and represents the spars and other internal structural components. At each incremental distance outboard of the aircraft centerline, the elastic axis assumes the equivalent EI and GJ values for the particular components that the distance represents (see Figure 2a).

The elastic axis is broken up into small segments called link lengths and in the analysis each link length is considered to be a cantilever beam (see Figure 2b). Each panel on the wing is assumed to be assigned to some segment of the elastic axis in a direction perpendicular to the elastic axis (see Figures 2b and 3). Attachment of the panel to a link length is accomplished by assuming an infinitely rigid arm connecting the panel center of pressure and the endpoint of the elastic segment. The term infinitely rigid, as used here, means that whatever rotations are induced in the elastic axis segment to which the jth panel is assigned, the jth panel also undergoes these same rotations. This infinitely rigid arm serves as a means to translate the load to the outboard point i on its attached elastic axis segment (see Figure 2b).

Calculation of the structural influence coefficients is facilitated by the use of influence coefficients internal to the program. These internal influence coefficients are called Elastic Axis Flexibility Vectors. They are found as follows. First, a unit force, unit moment and unit torque (with positive orientation) are placed at the outboard end of the ith link length (see Figure4). Second, with this unit loading condition, the rotations induced at the loaded point i are calculated by considering the variance in bending and torsional stiffness inboard of the loaded point. This procedure is repeated for every link length starting at the outboard end of the first segment and proceeding out the axis until the end is reached. This procedure is discussed in more detail in Section 4.

Every effort was made to make the program as general as possible. As a result, the position of an aerodynamic panel can be anywhere within a 360° arc from its assumed point of attachment on the elastic axis (see Figure 5a).

The center of pressure of the panel may have the same coordinates as its attachment point on the elastic axis if this is necessary (see Figure 5b). Discontinuities in the elastic axis can also be tolerated providing they are handled as the end of an elastic axis link length (see Figure 6). The link lengths may be as long or as short as desired and these lengths may vary from link to link.

A positive loading condition is illustrated in Figure 4. A positive force is up as a lift force. Torque is positive when it induces a positive angle of attack for the wing, and a positive moment tends to bend the wing upward.

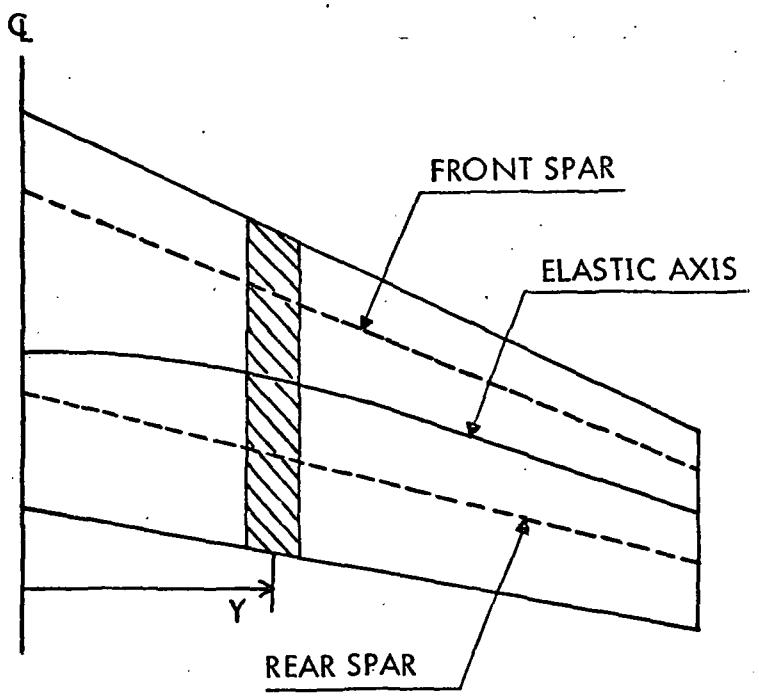

a) Shaded Area Shows Region Where Equivalent EI and GJ Are Found.

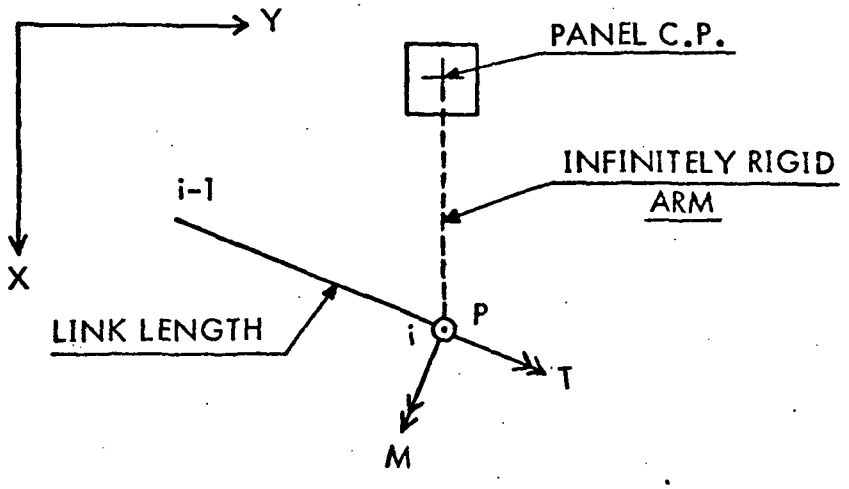

b) Panel Connection to Elastic Axis Link Length and Positive Loading Condition

Figure 2
Example of Elastic Axis, Link Length and Panel Arrangement.

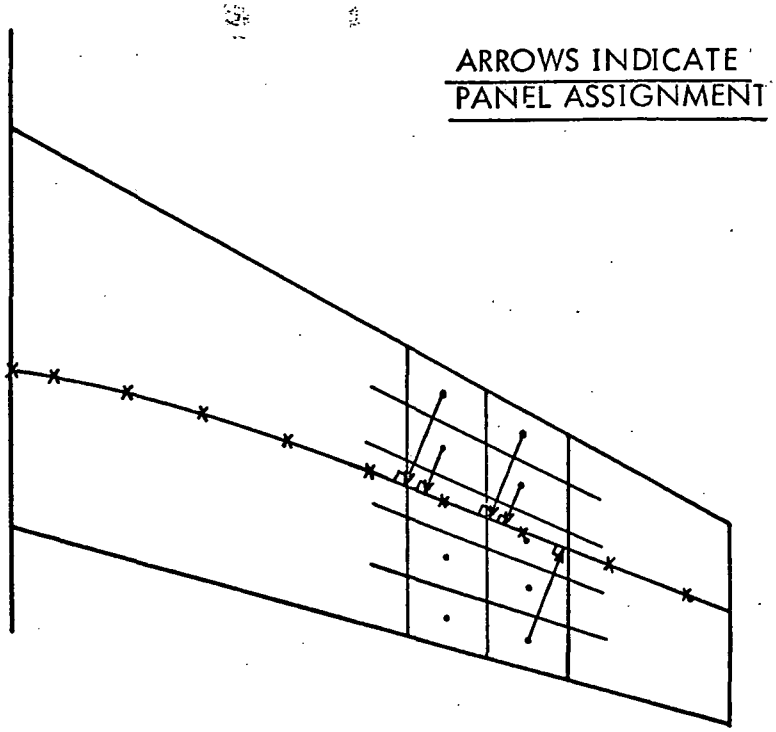

Figure 3 Examples of Panel Assignment to the Elastic Axis

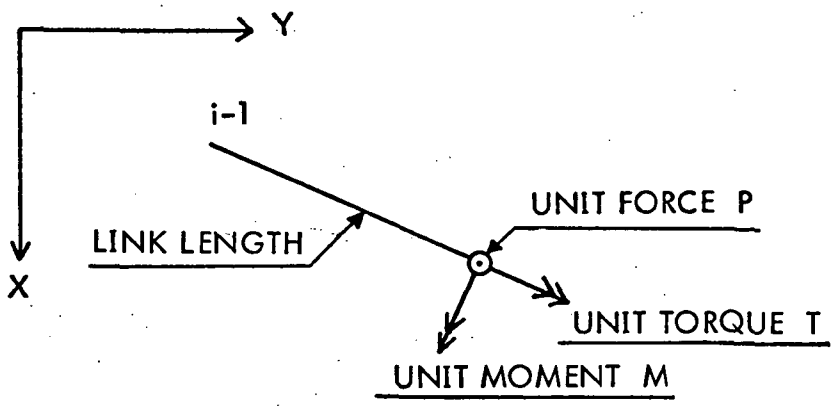

Figure 4 Description of Unit Loading Condition

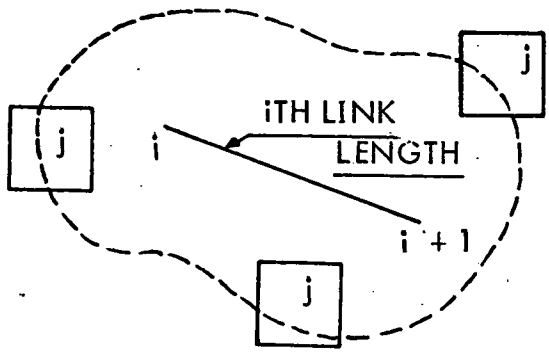

(a) Aerodynamic Panel j May Be Oriented Anywhere on the Arbitrary Arc Shown.

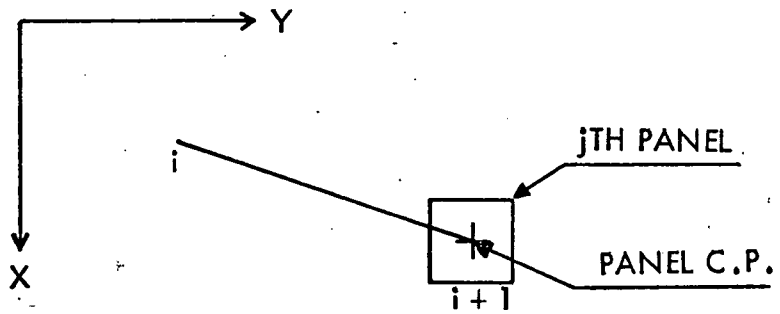

(b) Coordinates of the Panel Control Point May Be the Same as the Coordinate of the End of an Axis Segment.

Figure 5 Panel Assignment Possibilities

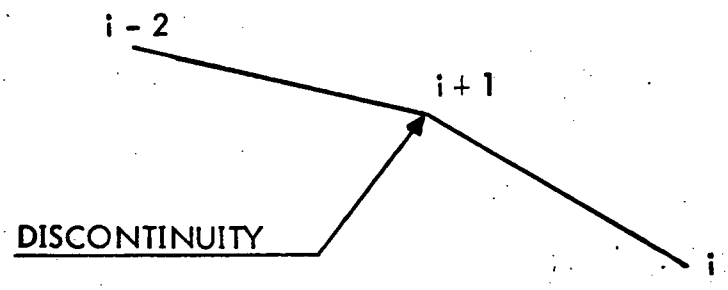

Figure 6 Discontinuities to be Handled as Segment End Points

4. METHOD OF ANALYSIS

This section gives a discussion of the step-by-step procedures used in calculating the structural influence coefficient matrix of wing-body-tail configuration. The procedure for the wing alone case is described in Paragraph 4.1. The procedure for the complete airplane case is described in Paragraph 4.2.

4.1 Method for Computing the Structural Influence Coefficient Matrix for the Wing

Calculation of the length of each elastic axis segment is the first computation completed by the program. This is done by considering each segment of the axis to be the hypotenuse of a right triangle. Then using the coordinates of each end of the segment whose length is to be calculated, the following relation is used:

$$L_{i-1} = \left[(x_i - x_{i-1})^2 + (y_i - y_{i-1})^2 \right]^{\frac{1}{2}} \qquad (1)$$

The coordinates used in Equation (1) are defined in Figure 7.

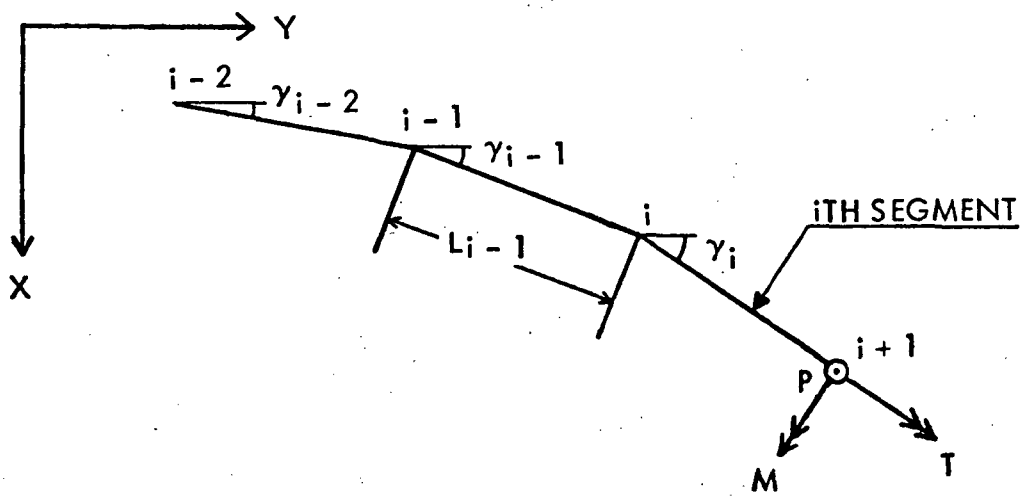

Figure 7 Unit Loading System on Elastic Axis

As stated in Section 3, calculation of the elastic axis flexibility vectors facilitates the computation of the structural influence coefficients for the aerodynamic panels. The procedure involves the placing of a unit force, unit moment and unit torque (with positive orientation) at the outboard end of the i-th segment of the elastic axis (see Figure 7).

The sweep angle for each elastic axis segment is found using the formula:

$$\gamma_{i-1} = \tan^{-1} \left[(x_i - x_{i-1}) / (y_i - y_{i-1}) \right] . \qquad (2)$$

The relative angle between any two segments of the elastic axis is the difference between two individual sweep angles (see Figure 8) and is expressed as:

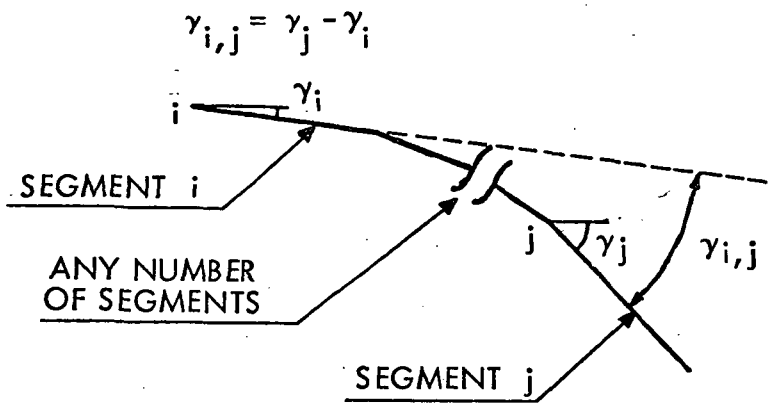

Figure 8 Relative Angle Between Segment i and Segment j

The rotation induced in a segment of the elastic axis by the unit loading system is found by transferring each component of the unit load system to the endpoint of the segment for which the rotation is desired. First, to transfer the unit force P from point i to point j + 1 on the elastic axis, a torque arm T and moment arm M must be found (see Figure 9).

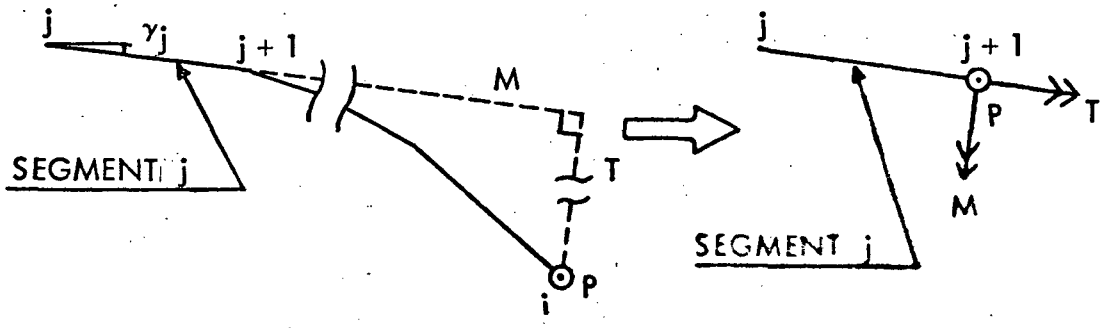

Figure 9 Transfer of Force P From Point i to Point j+1

The quantities T and M are determined as follows:

$$T = (y_i - y_{j+1}) \sin \gamma_j - (x_i - x_{j+1}) \cos \gamma_j \qquad (4a)$$

$$M = (y_i - y_{j+1}) \cos \gamma_j + (x_i - x_{j+1}) \sin \gamma_j \qquad (4b)$$

Thus the bending angle, θ_P, and twist angle, ϕ_P, at point j + 1 as induced by the unit load P at point i are given by the equations:

$$\theta_P = \frac{ML_j}{EI_j} + \frac{L_j^2}{2EI_j} \tag{5a}$$

$$\phi_P = \frac{TL_j}{GJ_j} \tag{5b}$$

The unit moment and unit torque are transferred from their point of application to the endpoint of the desired segment in a similar manner. A unit moment applied at point i produces a moment and a torque at point j + 1 as can be seen in Figure 10.

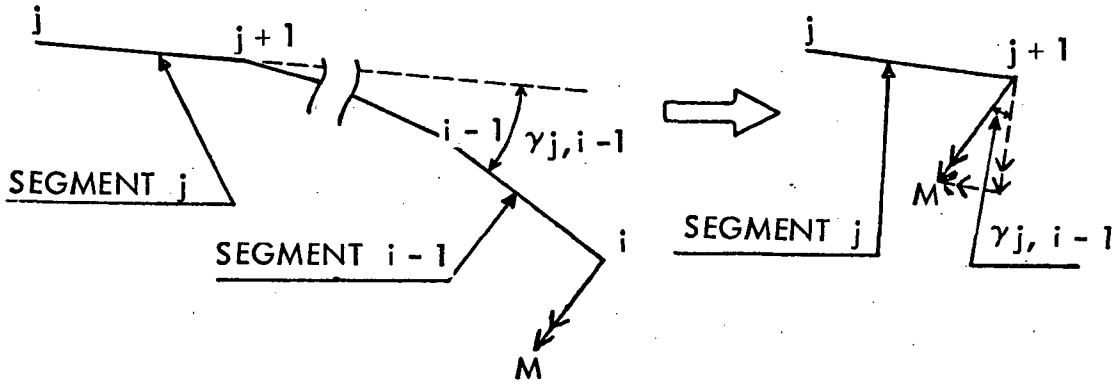

Figure 10 Transfer of Moment M From Point i to Point j+1

The bending angle, θ_M, and twist angle, ϕ_M, at point j + 1 due to a unit bending moment are now given by:

$$\theta_M = \frac{(\cos \gamma_{j,\, i-1})\ (L)}{EI_j} \tag{6a}$$

$$\phi_M = \frac{-(\sin \gamma_{j,\, i-1})\ (L)}{GJ_j} \tag{6b}$$

where $\gamma_{j,\, i-1}$ is the relative angle between segment j and segment i - 1 as shown in Figure 10.

The unit torque T applied at i is transferred in much the same way as the moment, giving the following equations for the bending angle θ_T and the twist angle, ϕ_T:

$$\theta_T = \frac{(\sin \gamma_{j,\,i-1})\ (L)}{EI_j} \tag{7a}$$

$$\phi_T = \frac{(\cos \gamma_{j,\,i-1})\ (L)}{GJ_j} \tag{7b}$$

The next step in the computer program is to project the angles of twist and bending into the streamwise direction, giving the change in streamwise rotation, $\Delta\alpha$ at the end-point $j+1$ of elastic axis segment j.

$$\Delta\alpha_{P_{j+1}} = \phi_P \cos \gamma_j - \theta_P \sin \gamma_j \qquad \text{(for unit force P)} \tag{8a}$$

$$\Delta\alpha_{M_{j+1}} = \phi_M \cos \gamma_j - \theta_M \sin \gamma_j \qquad \text{(for unit moment M)} \tag{8b}$$

$$\Delta\alpha_{T_{j+1}} = \phi_T \cos \gamma_j - \theta_T \sin \gamma_j \qquad \text{(for unit torque T)} \tag{8c}$$

The total streamwise rotation at any point on the elastic axis is simply the summation of the changes in rotation of all the points inboard of that point added to the change in rotation of that point. For example:

$$\alpha_{P_{j+1,\,i}} = \sum_{n=1}^{j+1} \Delta\alpha_{P_n} \qquad \text{(for unit force P at point i)} \tag{9a}$$

$$\alpha_{M_{j+1,\,i}} = \sum_{n=1}^{j+1} \Delta\alpha_{M_n} \qquad \text{(For unit moment M at point i)} \tag{9b}$$

$$\alpha_{T_{j+1,\,i}} = \sum_{n=1}^{j+1} \Delta\alpha_{T_n} \qquad \text{(for unit torque T at point i)} \tag{9c}$$

Equations 9a, 9b, and 9c represent the desired elastic axis flexibility vectors. These equations hold as long as $j + 1$ is less than or equal to i; that is, for all segments inboard of the loading point i. If $j + i$ is greater than i, then point $j + 1$ is outboard of point i, and the streamwise rotation of a point outboard of the loading point i is the same as that of point i.

Now that the elastic axis flexibility vectors (Equations 9) have been calculated, the structural influence coefficients can be calculated. First, an IASIGN vector is constructed which assigns each aerodynamic panel to an endpoint of the elastic axis (see Figure 11).

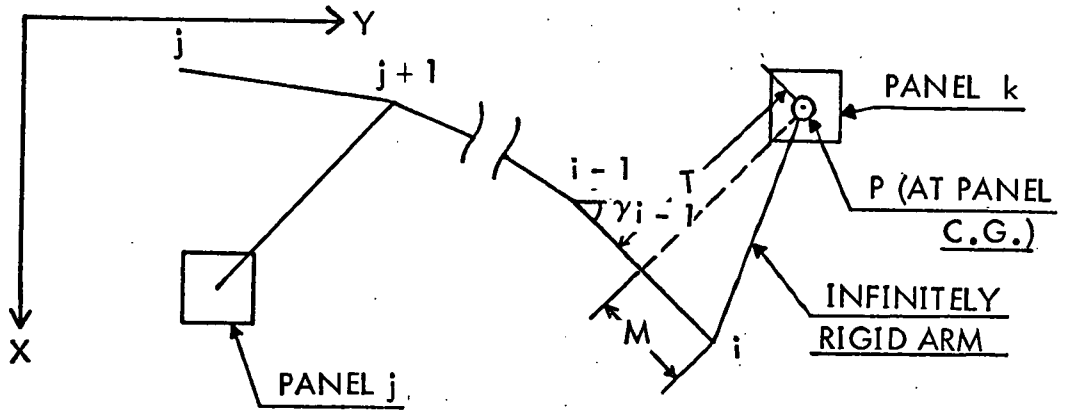

Figure 11 Panel Attachment to Assigned Point on the Elastic Axis

Construction of IASIGN involves judgment of how the actual structure should be interpreted in terms of the disjointed elastic axis and aerodynamic panel model which is used here. A unit load applied on any such panel K can be transferred to its assigned elastic axis endpoint i by finding the torque arm T and moment arm M as follows:

$$T = (y_k - y_i) \sin \gamma_{i-1} - (x_k - x_i) \cos \gamma_{i-1} \qquad (10a)$$

$$M = (y_k - y_i) \cos \gamma_{i-1} + (x_k - x_i) \sin \gamma_{i-1} \qquad (10b)$$

The streamwise rotation of the elastic axis can now be found by a linear combination of the elastic axis flexibility vectors of Equations (9). The rotation of any panel j due to the unit load on panel k is the same as the rotation of the endpoint of the elastic axis to which panel j is assigned. Therefore, if panel j is assigned to point $j + 1$ and panel k to i,

$$C_{jk} = \alpha_{P_{j+1,i}} + M \cdot \alpha_{M_{j+1,i}} + T \cdot \alpha_{T_{j+1,i}} \qquad (11)$$

where M and T are the moment arm and torque arm found from Equation (10); and $\alpha_{P_{j+1,i}}$, $\alpha_{M_{j+1,i}}$, and $\alpha_{T_{j+1,i}}$ are the elastic axis flexibility vectors as found in Equations (9).

By using the preceding method, systematically for all panels, the complete structural influence coefficient matrix is calculated. All panels assigned to the same elastic axis endpoint will have the same streamwise rotation. All panels assigned to endpoints outboard of the endpoint to which the loaded panel is assigned will have the same rotation as the loaded panel.

The last operation carried out by the structural program is to return the influence coefficient matrix to the mainline to be used in the aero-elastic analysis.

4.2 Method for Computing the Structural Influence Coefficient Matrix for Wing-Body-Tail Combinations

For the purpose of computing the structural influence coefficient matrix of a wing-body-tail combination, the fuselage is assumed to be represented by a straight torsionally rigid beam. The tail surface and wing are represented by an elastic axis as shown in Figure 12. The vertical tail is assumed ideally rigid.

The computer program was developed by adopting the following assumptions:

(1) The point of intersection of the wing elastic axis and the fuselage elastic axis is assumed to be locally rigid. See point A of Figure 12.

(2) Any load on the wing does not affect any part of the fuselage or the horizontal tail. This is due to the first assumption.

(3) The bending deflection of the front fuselage elastic axis (i.e. from nose to point A) affects the wing only in a region between the wing leading edge and the wing elastic axis. The influence of the fuselage angular deflection is assumed to decrease linearly from the wing root chord with full deflection to a distance at half the structural root chord c_s where no influence of the fuselage angular deflection is assumed. Thus, as shown in Figure 12, only region D of the wing is affected by the front fuselage deflection. With the coordinate systems shown in Figure 12, the angular deflection at any point P' in region D due to the front fuselage deflection is given by:

$$\Delta\alpha_{P'} = (\Delta\alpha_{root}) \frac{(\frac{c_s}{2}) - y'}{(\frac{c_s}{2})} \; ; \; y' \leq \frac{c_s}{2} \qquad (12)$$

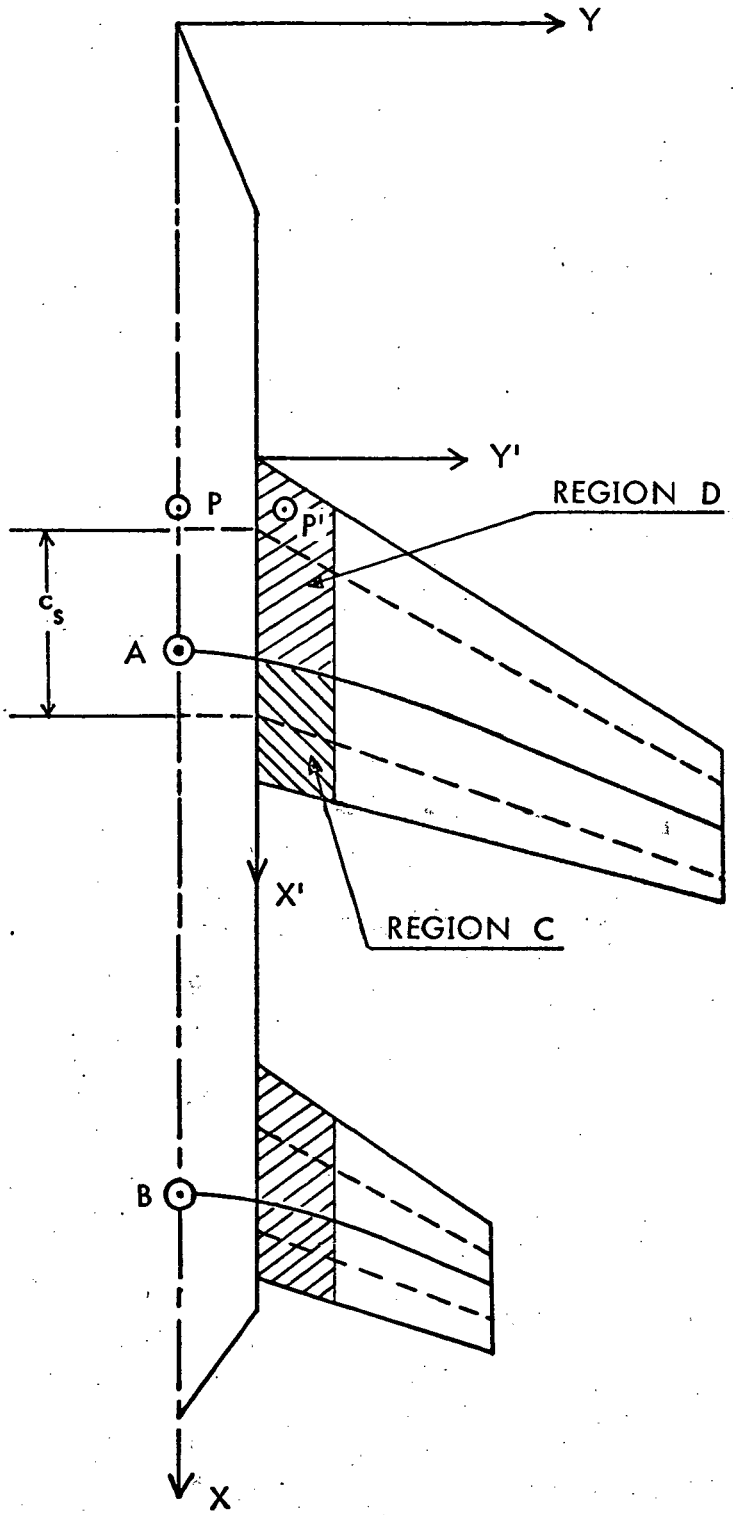

Figure 12 Structural Schematic for Wing-Body-Tail Program

where $\Delta\alpha_{root}$ is the angular deflection at the wing root chord and is assumed the same as $\Delta\alpha_P$ at a corresponding point P (i.e., $y_P = y_{P_1}$) on the fuselage elastic axis. In the computer program, $\Delta\alpha_P$ is computed by linear interpolation between end-points of the fuselage elastic-axis segments. Note that the actual deflection at any point on the wing surface is obtained by super-imposing the fuselage effect on the wing alone case.

(4) The same assumption on the influence of the aft fuselage deflection applies also to the rear part of the wing surface. See region C of Figure 12.

(5) Any load on the tail surface is first transferred to point B and the fuselage deflection is then computed by using beam theory. The fuselage deflection affects the horizontal tail in two ways. The first is that the angular deflection at point B is carried over to the whole tail surface and the second is that the tail surface at the junction will follow the fuselage in bending. This last effect can be computed by assumption (3). For an all-movable tail, this last effect does not exist and this is recognized in the program by an 'if' statement.

The computer program was written in such a way that efficient and repetitive use of the wing-alone structural program can be made. Therefore, the complete structure is divided into three parts with symbols in parentheses: the fuselage (F), wing (W), and the horizontal tail (T). If C_{jkFW} represents the angular deflection in the flight direction at panel j on the fuselage due to a unit load on panel k of the wing surface, with similar definitions for other symbols, then it can be shown that many elements in the structural influence coefficient matrix are zero. For example, $C_{jkFW} = 0$ and $C_{jkTW} = 0$ for all j and k. Most elements in C_{jkWF} and C_{jkWT} are also zero. Most elements in C_{jkFF} are zero because the front fuselage does not affect the aft fuselage and vice versa. The complete structural influence coefficient matrix can therefore be expressed as a partitioned matrix shown below:

$$\begin{bmatrix} [C_{jkFF}] & [0] & [C_{jkFT}] \\ [C_{jkWF}] & [C_{jkWW}] & [C_{jkWT}] \\ [C_{jkTF}] & [0] & [C_{jkTT}] \end{bmatrix}$$

5. VALIDATION OF THE [C] MATRIX SUBROUTINE

To test the validity and accuracy of the [C] matrix subroutine, a total of four examples were tested. Two of these test cases are presented here. The first, a NACA box beam (Reference 2) was used to test the wing-only [C] matrix program. This test case is described in Section 5.1. The second test case, a simple elastic axis model, was used to test the wing-body-tail [C] matrix program and is described in Section 5.2.

5.1 Wing-Only Test Case

The thin-walled box beam (Figure 13) presented in Reference 2, was the first test wing examined. Figure 14 shows the geometry of the wing and the elastic axis location. Figure 15 shows the EI and GJ distributions used. The value of GJ was assumed to be infinite in the carry-through section of the box beam, since the mounting of the test wing allowed bending but no twisting in this section. A comparison of the computed rotations with the experimental results is shown in Figure 16. It is seen that the largest discrepancy is of the order of .001 rad (or .0573 degrees). This discrepancy is judged to be sufficiently small to consider the program to be working properly. It must be kept in mind that it is not possible to state whether the discrepancy is caused by some slight error in the computer program or by the beam idealization used in the program.

5.2 Wing-Body-Tail Case

No usable test data were available on an actual wing-body-tail configuration. For that reason, the computer logic of the extended $[C]$ matrix subroutine was checked by performing a computation by hand for a simple wing-body-tail combination as shown in Figure 17. The coordinates of control points and elastic axis endpoints are shown in Table 1 and 2, respectively. The assumed EI and GJ values for each elastic axis segment are presented in Table 3. The angular changes in the flight direction (i.e. $\Delta\alpha$) at various locations due to a unit load at some point are tabulated in Table 4. As can be seen from Table 4, the computer program produced the same numerical results as computed by hand. The computer program is, therefore, considered to be correct.

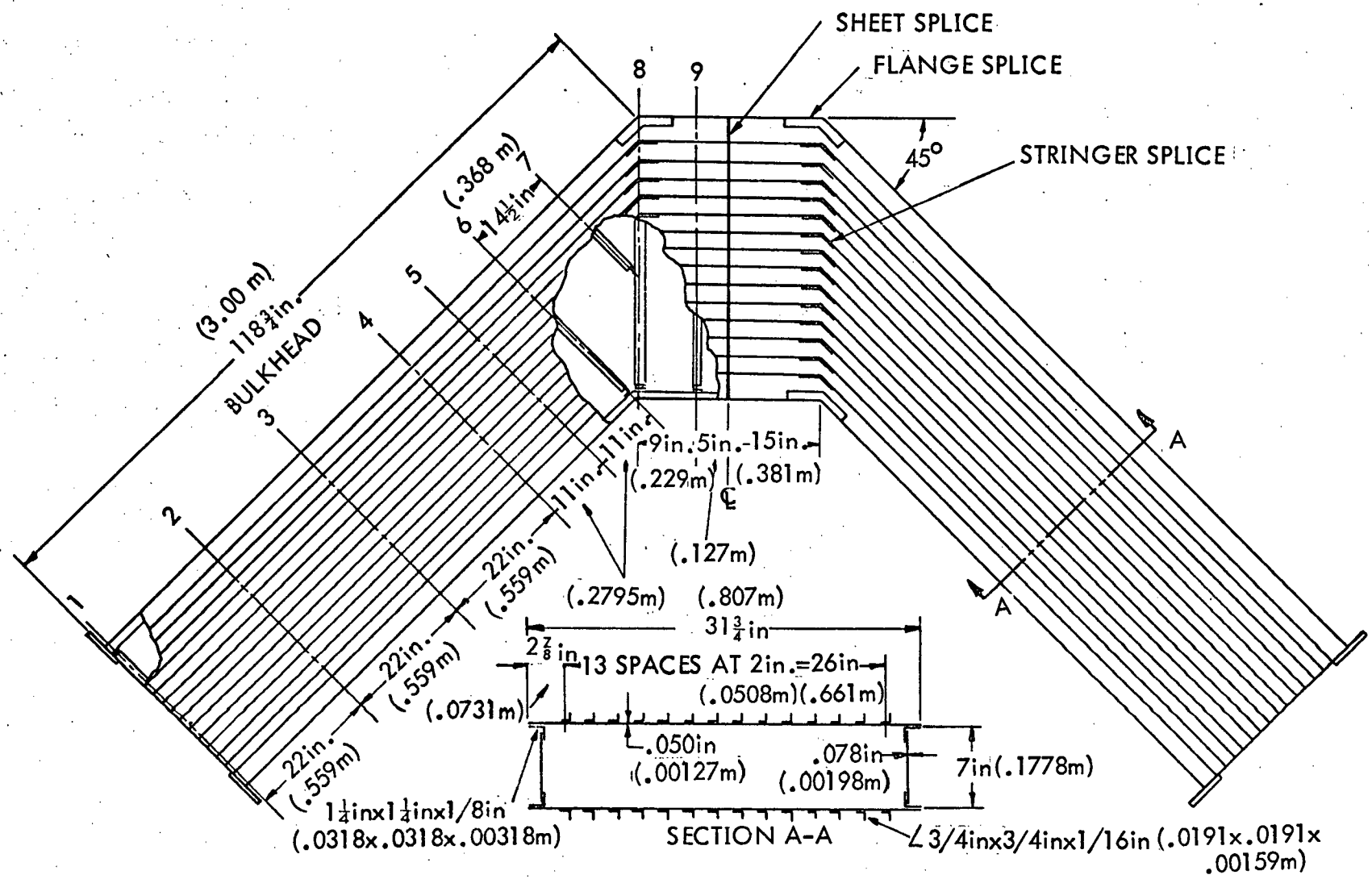

Note: Data from Reference 2

Figure 13 Details of the Box Beam

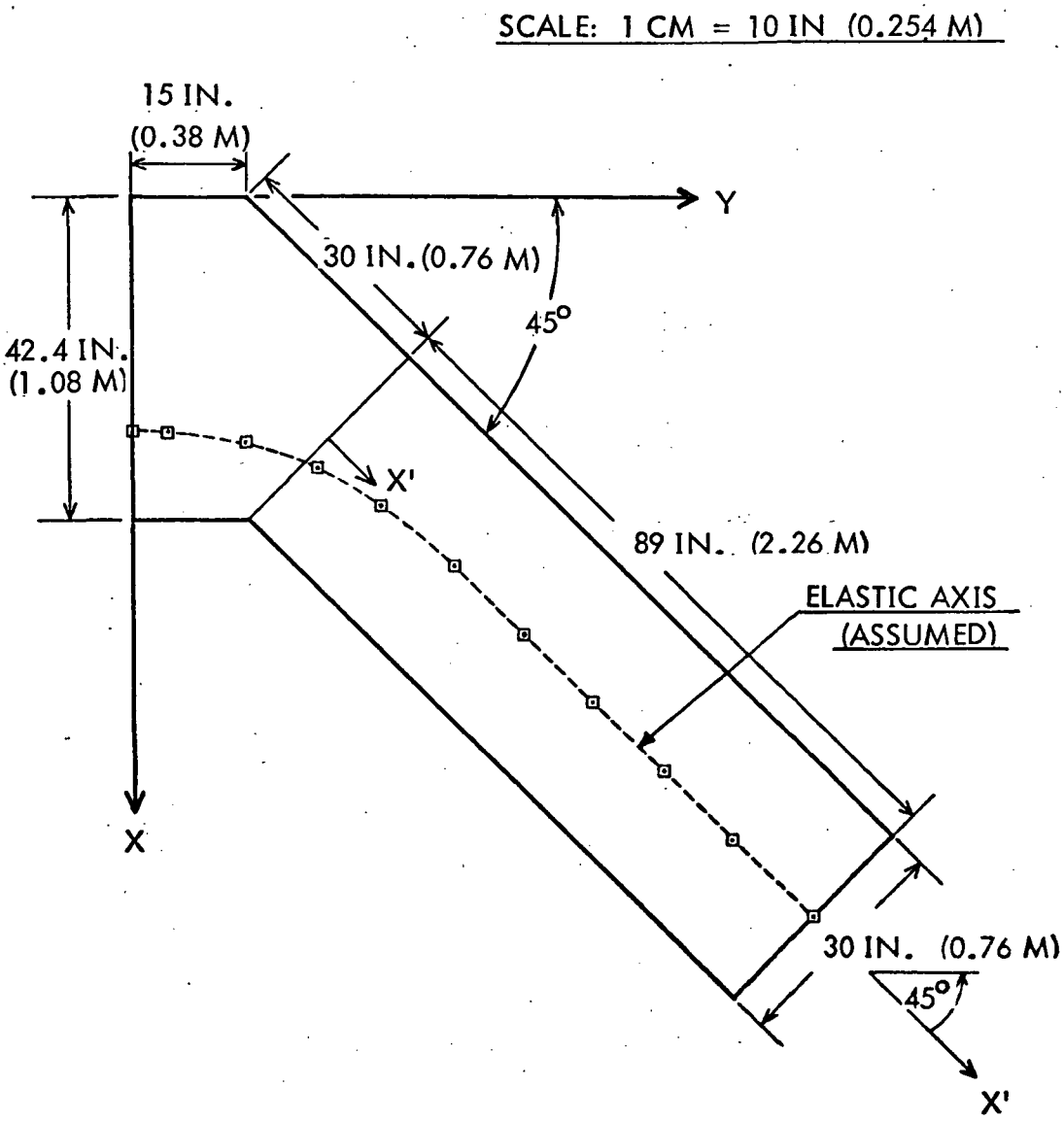

Figure 14 Planform Definition of the Box Beam

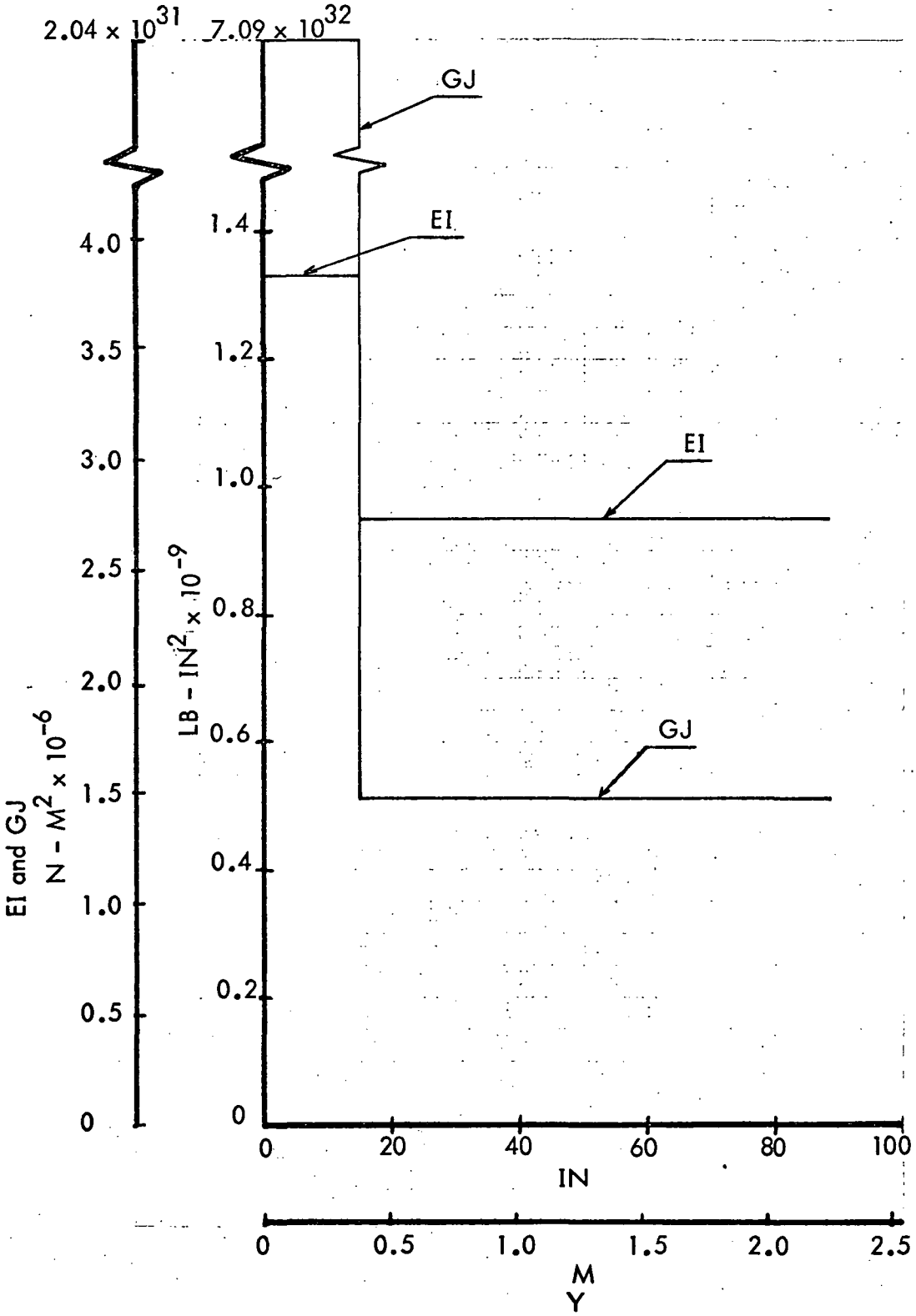

Figure 15 EI and GJ Distribution for the Box Beam

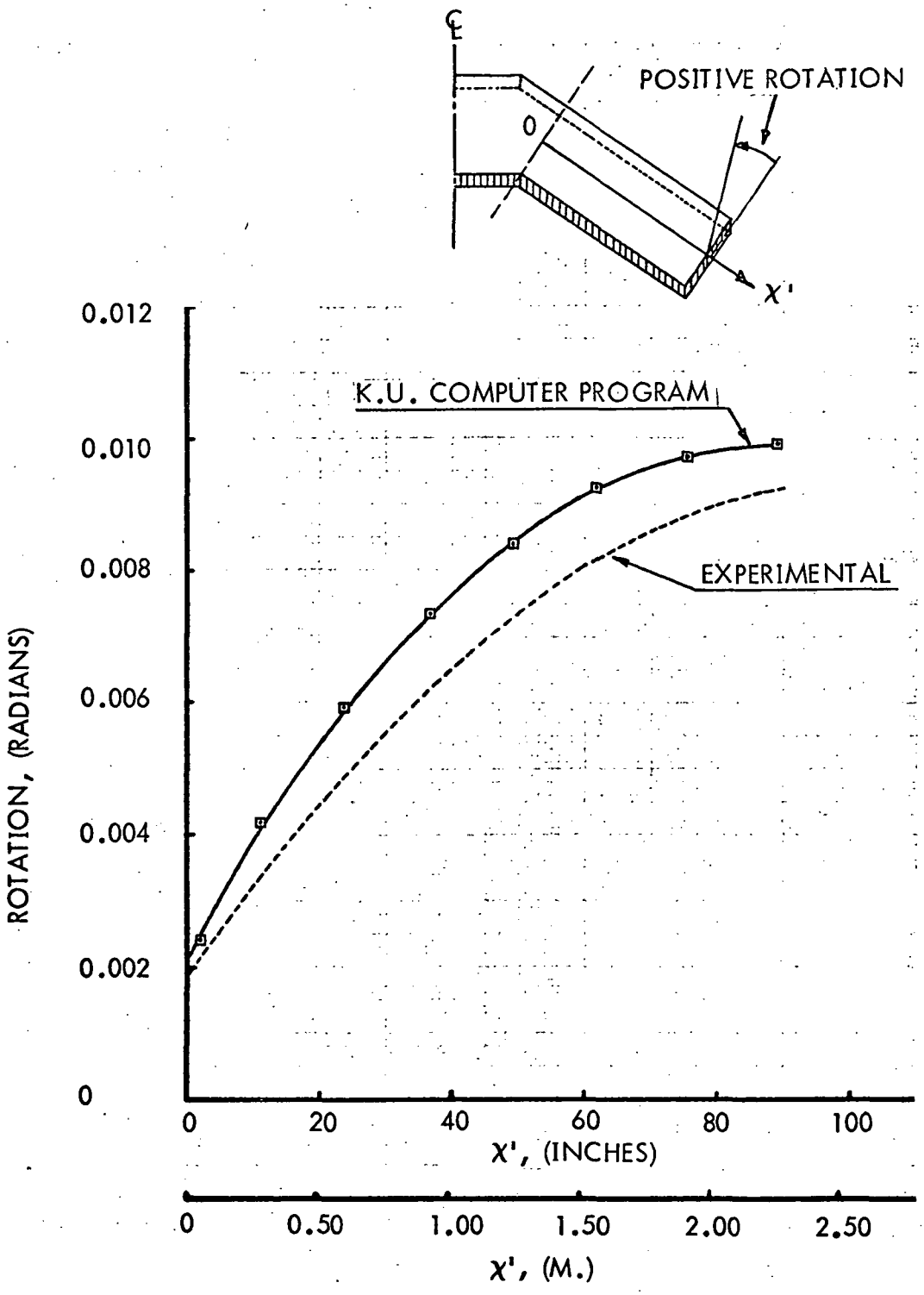

Figure 16. Distortion of the Box Beam for Tip Bending Load

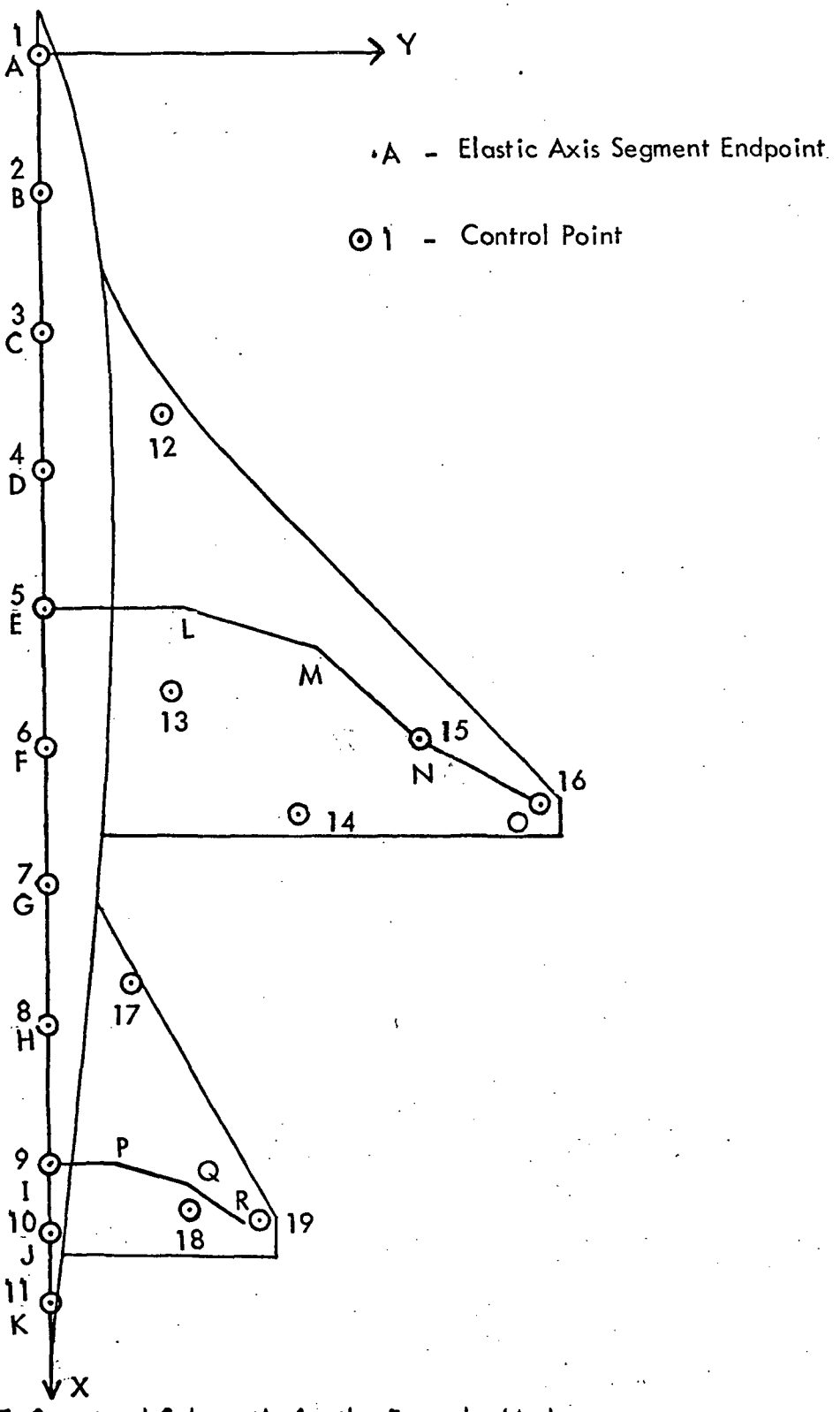

Figure 17 Structural Schematic for the Example Airplane

TABLE 1 CONTROL POINT COORDINATES FOR FIGURE B.17

POINT	X(in.)	(m)	Y(in.)	(m)
1	0.0	0.0	0.0	0.0
2	10.0	0.254	0.0	0.0
3	20.0	0.508	0.0	0.0
4	30.0	0.762	0.0	0.0
5	40.0	1.016	0.0	0.0
6	50.0	1.270	0.0	0.0
7	60.0	1.524	0.0	0.0
8	70.0	1.778	0.0	0.0
9	80.0	2.032	0.0	0.0
10	85.0	2.159	0.0	0.0
11	90.0	2.286	0.0	0.0
12	26.0	0.661	8.5	0.216
13	46.0	1.168	9.0	0.2285
14	55.0	1.396	18.0	0.457
15	49.66	1.261	26.73	0.679
16	54.66	1.386	35.39	0.899
17	67.0	1.701	6.0	0.1523
18	83.5	2.120	10.0	0.254
19	84.303	2.141	15.0	0.381

Notes: Main Wing Structural Root Chord- 50.in.(1.270 m.)

Horizontal Tail Structural Chord = 20.in. (0.508 m.)

Half-Width of Fuselage at Main Wing = 5.in. (0.127 m.)

Half-Width of Fuselage at Horizontal Tail = 2.in. (0.0508 m.)

TABLE 2 ELASTIC AXIS ENDPOINT COORDINATES FOR FIGURE 17

POINT	X (in.)	(m)	Y (in.)	(m)
A	0.0	0.0	0.0	0.0
B	10.0	0.254	0.0	0.0
C	20.0	0.508	0.0	0.0
D	30.0	0.762	0.0	0.0
E	40.0	1.016	0.0	0.0
F	50.0	1.270	0.0	0.0
G	60.0	1.524	0.0	0.0
H	70.0	1.778	0.0	0.0
I	80.0	2.032	0.0	0.0
J	85.0	2.159	0.0	0.0
K	90.0	2.286	0.0	0.0
L	40.0	1.016	10.0	0.254
M	42.59	1.082	19.66	0.499
N	49.66	1.261	26.73	0.679
O	54.66	1.388	35.39	0.899
P	80.0	2.032	5.0	0.127
Q	81.294	2.065	9.8295	0.250
R	84.303	2.141	13.8225	0.351

TABLE 3 ASSUMED EI AND GJ VALUES FOR ELASTIC AXIS SEGMENTS FOR FIGURE 17

SEGMENT	EI (lb-in^2)	(N-m^2)	GJ (lb-in2)	(N-m2)
A-B	2.0×10^{10}	5.74×10^{7}	*	*
B-C	4.0×10^{10}	1.148×10^{8}	*	*
C-D	5.0×10^{10}	1.435×10^{8}	*	*
D-E	5.0×10^{10}	1.435×10^{8}	*	*
E-F	5.0×10^{10}	1.435×10^{8}	*	*
F-G	5.0×10^{10}	1.435×10^{8}	*	*
G-H	4.0×10^{10}	1.148×10^{8}	*	*
H-I	3.0×10^{10}	8.62×10^{7}	*	*
I-J	2.0×10^{10}	5.74×10^{7}	*	*
J-K	1.0×10^{10}	2.87×10^{7}	*	*
E-L	1.0×10^{9}	2.87×10^{6}	8.0×10^{8}	2.295×10^{6}
L-M	8.0×10^{8}	2.295×10^{6}	6.0×10^{8}	1.722×10^{6}
M-N	5.0×10^{8}	1.435×10^{6}	3.0×10^{8}	8.62×10^{5}
N-O	2.0×10^{8}	5.74×10^{5}	1.0×10^{8}	2.87×10^{5}
I-P	3.0×10^{8}	8.62×10^{5}	2.0×10^{8}	5.74×10^{5}
P-Q	2.0×10^{8}	5.74×10^{5}	1.0×10^{8}	2.87×10^{5}
Q-R	1.0×10^{8}	2.87×10^{5}	5.0×10^{7}	1.435×10^{4}

* Fuselage is assumed torsionally rigid ($GJ = \infty$)

TABLE 4 COMPARISON OF RESULTS BY HAND COMPUTATION AND COMPUTER PROGRAM FOR $\Delta\alpha$ ($\times 1\ 0^{8}$ radian)

LOADED POINT			1	2	3	4	6	8	11	19
DEFLECTED POINT	12	HAND	0.77400	0.53320	0.29240	0.86000				
		COMPUTER	0.77400	0.53320	0.29240	0.86000				
	13	HAND					-0.050400		-0.45360	
		COMPUTER					-0.050400		-0.45360	
	14	HAND					-0.048000		-0.60000	
		COMPUTER					-0.048000		-0.60000	
	15	HAND					-0.012635		-0.11372	
		COMPUTER					-0.012635		-0.11372	
	17	HAND						-0.90250	-2.3125	-12.650
		COMPUTER						-0.90250	-2.3125	-12.649
	18	HAND							-2.7513	-25.849
		COMPUTER							-2.7513	-25.849
	19	HAND							-2.7250	-30.542
		COMPUTER							-2.7250	-30.542

6. REFERENCES

1. Roskam, J., Lan, C., and Mehrotra, S.; "A Computer Program for Calculating α- and q- Stability Derivatives and Induced Drag for Thin Elastic Aeroplanes at Subsonic and Supersonic Speeds," NASA CR-112229; Prepared under NASA Grant NGR 17-002-071 by the Flight Research Laboratory of the Department of Aerospace Engineering of the University of Kansas, October, 1972. Appendix A of the Summary Report, NASA CR-2117.

2. Zender, G., and Libove, C., "Stress and Distortion Measurements in a 45° Swept Box Beam Subjected to Bending and Torsion," NACA TN-1525, March, 1948.